EVALUATION OF SHEAR DESIGN METHODS FOR LARGE, LIGHTLY-REINFORCED CONCRETE BEAMS

E.G. Sherwood, E.C. Bentz and M.P. Collins
Department of Civil Engineering, University of Toronto, 35 St. George St., Toronto, Ontario, Canada M5S 1A4
E-mail: sherwoo@ecf.utoronto.ca

Abstract

This paper describes one phase of an extensive experimental program that has recently been completed at the University of Toronto. In this phase, eighteen lightly-reinforced shear-critical reinforced concrete beams were loaded to failure. The abilities of the ACI-318 shear design method and a simplified design method based on the Modified Compression Field Theory to predict the failure loads are compared. It is found that the ACI design method is dangerously unconservative when applied to large beams and one-way slabs constructed without stirrups, while the simplified MCFT design method is both safe and accurate. Studies of the mechanism of shear transfer indicate that approximately one quarter of the shear in a reinforced concrete beam constructed without stirrups is transferred in the compression zone, with the rest carried primarily by aggregate interlock. The development of theoretically-sound shear design methods must therefore be based on the fact that aggregate interlock plays a critical role in the shear behaviour of reinforced concrete structures.

Introduction

It has long been a goal of code writers to improve the quality of reinforced concrete design procedures for shear. Unlike flexural failures, shear failures in reinforced concrete are brittle and sudden, and occur with little or no warning. Furthermore, they are less predictable than flexural failures, due to considerably more complex failure mechanisms. While flexural design provisions are based on the rational assumption that plane sections remain plane, the search for equally rational design provisions for shear continues.

Figure 1: ACI and CSA Design Codes

The recently updated and reissued ACI-318-05 and CSA A23.3-04 Design Codes for Concrete (Figure 1) represent the culmination of extensive research involving all aspects of the behaviour of reinforced concrete. However, the shear design provisions in the ACI code remain based on traditional empirical relationships developed over 40 years ago, and do not reflect the vast improvements in understanding of the shear behaviour of reinforced concrete that have been gained over that time. In particular, there are significant concerns that the ACI shear design provisions are unconservative when applied to large beams and one-way slabs constructed without stirrups. As such, they must be replaced with rational, theoretically-sound design provisions that can predict the shear behaviour of these brittle, complex structural elements.

A particular aspect of the shear behaviour of reinforced concrete that is deserving of additional attention is the effect of the maximum aggregate size on the shear response of reinforced concrete sections. This is particularly true for reinforced concrete beams constructed without stirrups, since aggregate interlock is the dominant mechanism of shear transfer in these element types. Increasing the size of the coarse aggregate produces rougher cracks that are better able to transfer shear stresses. Likewise, reducing the maximum aggregate size decreases the shear strength of a concrete section. Furthermore, the use of high

M. Pandey et al. (eds), Advances in Engineering Structures, Mechanics & Construction, 153–164.

strength concrete or low-density aggregate can result in fracturing of the coarse aggregate particles as cracks form, thereby producing smoother cracks with a greatly reduced aggregate interlock capacity.

The Modified Compression Field Theory (MCFT) (Vecchio and Collins, 1985) employs equilibrium, compatability and experimentally verified stress-strain relationships to model the shear behaviour of cracked concrete. A fundamental relationship in the MCFT relates the shear stress on a crack surface due to aggregate interlock to the crack's width, the maximum aggregate size and the concrete strength. The aggregate effect was first codified when a general method of shear design was derived based on the MCFT and implemented in the AASHTO-LRFD bridge design guidelines. In 1994 the general method of shear design was implemented in the CSA concrete design code for buildings. Recently, an updated and simplified version of the general method has been developed (Bentz et al., 2005) and implemented in the 2004 CSA design code. The new general method, referred to as the Simplified Modified Compression Field Theory (SMCFT) has been found to be simpler than the original general method with, in many cases, improved predictive capabilities (Sherwood et al., 2005a).

As might be expected, there are certain areas of considerable disagreement between modern shear design methods based on the MCFT and the ACI method. The fundamental question that must be asked, therefore, is: "Are the existing ACI shear design methods sufficiently safe, such that a reworking of the provisions is not necessary". The corollary to this question is: "Has our understanding of the fundamental behaviour of reinforced concrete in shear advanced to such a stage such that modern shear design methods represent a clear improvement over traditional design methods?" The purpose of this paper is to explore the answers to these questions by studying the behaviour of reinforced concrete beams in shear, focusing on the role played by the coarse aggregate. A significant experimental program will be presented in which eighteen shear critical concrete beams constructed with different maximum aggregate sizes were tested to failure. The SMCFT design method will be discussed, and its predictive capabilities will be compared to those of the empirical ACI shear design method.

ACI Method of Shear Design

Morsch (1909) was amongst the first to research the behaviour of reinforced concrete in shear. At the beginning of the 20th century he developed the well-known 45° truss model, whereby shear was visualized to be transferred through the web of a cracked concrete member through a field of diagonal compression in the concrete and tension in transverse reinforcement. To produce an expression for the shear strength of a concrete section, he assumed that shear cracks that formed did so at an angle, θ, of 45°:

$$v = \frac{V}{b_w jd} = \frac{A_v f_v}{b_w s} \tag{1}$$

Reflecting the design philosophy at the time, f_v was taken to be the safe working stress in the stirrups. While Morsch knew from observations that failure shear cracks did not necessarily form at 45°, he saw no way to calculate the angle of what he termed secondary inclined cracks.

The 45° truss model entered use in various design methods and still forms the basis for the ACI expression for the shear resistance provided by stirrups. (The current ACI expression has simplified the equation by replacing the term jd with d.) As its use became more widespread, however, it was criticized for being overly conservative. In particular, the model assumed that only transverse reinforcement is effective at carrying shear, thereby predicting that a section without stirrups or bent-up bars would have no shear strength whatsoever. Clearly this is not the case. Extensive research efforts were undertaken in order to ascertain the so-called "concrete contribution" to shear resistance, which was eventually set at an empirically derived safe working shear stress of $v_c=0.03f'_c$. For the first time, the shear resistance of a reinforced concrete section was divided up into two components: a concrete contribution (V_c) and a web reinforcement contribution (V_s) predicted by the 45° truss model:

$$V = V_c + V_s \tag{2}$$

This method was used to design numerous concrete structures in the post-war construction boom of the 1950s and early 1960s. In 1955, however, a considerable portion of the roof of the Wilkins Air Force Warehouse in Selby, Ohio collapsed. The collapsed portions of the beams supporting the roof had been designed without stirrups, assuming that they could safely resist a working shear stress of 0.6MPa (90psi = 0.03 x 3000psi specified concrete strength). However, failure occurred at a shear stress of approximately 0.5MPa (70psi), corresponding to only about 80% of the safe service load on the roof. It therefore became apparent that unsafe designs could result from what had previously been considered to be a safe, conservative method.

As a result of the warehouse collapse, extensive research was undertaken to derive a better expression for V_c. In 1962, these efforts resulted in what was believed to be a simple, conservative expression for the failure shear based on a purely empirical curve-fit through 194 experimental data points (ACI Committee 326, 1962). This well-known expression (Equation 3) entered design use through incorporation into the 1963 American Concrete Institute Design Code, and has remained essentially unchanged since that time:

$$V_c = 0.167\sqrt{f'_c}\, b_w d \quad \text{(MPa units)} \tag{3a}$$

$$V_c = 2\sqrt{f'_c}\, b_w d \quad \text{(psi units)} \tag{3b}$$

The Size Effect in Shear

Beams

At the time Equation (3) was developed, it was not understood that the failure shear stress for members constructed without web reinforcement decreases as the member depth increases in a phenomenon known as the "size effect." Unfortunately, the average height of the specimens tested to develop Equation (3) was 340mm. As a result, the original researchers did not notice a size effect in their tests, and the ACI expression predicts a continuous and linear increase in shear capacity as the beam depth increases. Equation (3), while originally intended to be a conservative estimate, is therefore unconservative for deeper members constructed without web reinforcement because it can not predict this size effect. The failure of the warehouse beams was attributed to an unexpected tensile force in the beams, while it is far more likely that it was simply a result of the size effect (Lubell et al., 2004).

The MCFT predicts that the size effect in shear is related to the crack spacing in the web and the crack widths. As discussed by Sherwood et al. (2004): "…the larger crack widths that occur in larger members reduce aggregate interlock. Crack widths increase nearly linearly both with the tensile strain in the reinforcement and with the spacing between cracks…for the same reinforcement strain, doubling the depth of the beam will double the crack widths at mid-depth. To maintain beam action, a shear stress equal to about V/b_wd must be transmitted across these cracks. The shear stress that can be transmitted across such cracks, however, decreases as the crack width increases and as the maximum aggregate size decreases." Thus, the limiting stress that can be transferred across cracks due to aggregate interlock in deep members is reached at a lower shear stress than in equivalent small beams. Once the limiting stress is reached, equilibrium cannot be maintained, and failure occurs.

The use of at least the minimum quantity of stirrups will largely eliminate the size effect by allowing more closely spaced cracks to form and by preventing the loss of aggregate interlock as the cracks widen. Web reinforcement consisting of additional longitudinal steel placed in layers along the height of a beam will also reduce the size effect. In this case, the size effect is related to the vertical spacing of the layers of reinforcement, rather than the overall height of the beam.

One-Way Slabs

To avoid the risk of a brittle shear failure, the ACI code requires that beams be constructed with stirrups if the factored shear force V_f exceed $\frac{1}{2}\phi V_c$. This requirement is relaxed for one-way slabs, however, as the code requires stirrups for these elements only when V_f exceeds the full value of ϕV_c. Yet it has been

shown in an extensive companion research program that the web width (b_w) has no effect on the failure shear stress of reinforced concrete flexural members (Sherwood et al., 2005b). As such, deep one-way transfer slabs in high-rise construction are particularly vulnerable to the size effect if designed using the ACI code, as the designer may wish to proportion the slab such that no stirrups are required.

Aggregate Effects

Early attempts in the 1950s to develop rational theories of reinforced concrete in shear neglected the role played by aggregate interlock. Both implicit and explicit in these early theories was the assumption that all the vertical shear force in concrete sections without transverse reinforcement is carried in the uncracked concrete compression zone. This represented a reasonable first approximation of the complex behaviour of these element types. As research progressed, however, a belief gradually emerged that significant shear stress may, in fact, be transferred through the cracked web of a reinforced concrete beam. Fenwick and Pauley (1968) definitively showed this to be the case. Through direct measurement on subassemblies, it was possible to conclude that at least 60% of the vertical shear is carried by aggregate interlock at flexural cracks, with the remaining proportion being carried in the compression zone and through dowel forces.

Despite the successes of early classic studies on aggregate interlock, their results have been forgotten or otherwise neglected by many prominent modern shear researchers. Tureyn and Frosch (2003), for example, have formulated an expression for V_c based on the explicit assumption that all of the vertical shear force is carried in the compression zone, describing the assumption as a "reasonable approximation." Many others have taken similar approaches, particularly those using fracture mechanics principles (for example, Bazant and Yu, 2005). The fact that the importance of aggregate interlock is not appreciated has slowed the implementation of theoretically-sound design methods for shear. In particular, the size effect in shear can not be adequately accounted for unless aggregate interlock is explicitly considered.

A Modern Method of Shear Design

A considerable step forward in shear design methods was the development of a general method of shear design based on the MCFT. Design methods based on the MCFT have a firm theoretical base and are not derived by empirical curve fits to experimental data. As such, MCFT-based shear provisions are able to predict the behaviour of reinforced concrete elements in shear where no experimental data is available. Particular strengths of MCFT-based shear design methods include the ability to accurately predict the size and aggregate effects.

The recently developed SMCFT (Bentz et al., 2005) is based on the methods in the AASHTO-LRFD and the 1994 CSA Standards, but has been considerably simplified. Simple expressions have been developed for β, the crack angle, θ and the longitudinal strain in the web, ε_x, thereby eliminating the need to iterate to solve for these values.

The SMCFT employs the following relationship to determine the shear resistance of a concrete section:

$$V = V_c + V_s = \beta\sqrt{f'_c}\, b_w d_v + \frac{A_v f_y}{s} d_v \cot\theta \tag{4}$$

The term β in Equation (4) is a parameter that models the ability of cracked concrete to transfer shear. It is a function of 1) the longitudinal strain at the mid-depth of the web, ε_x, 2) the crack spacing at the mid-depth of the web and 3) the maximum coarse aggregate size, a_g. It is calculated using an expression that consists of a strain effect term and a size effect term:

$$\beta = \frac{0.40}{(1+1500\varepsilon_x)} \cdot \frac{1300}{(1000+s_{ze})} = (\text{strain effect term}) \cdot (\text{size effect term}) \tag{5}$$

The longitudinal strain at the mid-depth of a beam web is conservatively assumed to be equal to one-half the strain in the longitudinal tensile reinforcing steel. For sections that are neither prestressed nor subjected to axial loads, ε_x is calculated by:

$$\varepsilon_x = \frac{M_f/d_v + V_f}{2E_s A_s} \tag{6}$$

The effect of the crack spacing at the beam mid-depth is accounted for by use of a crack spacing parameter, s_z. This crack spacing parameter is equal to the smaller of either the flexural lever arm (d_v=0.9d or 0.72h, whichever is smaller) or the maximum distance between layers of longitudinal crack control steel distributed along the height of the web. To be effective, the area of the crack control steel in a particular layer must be greater than $0.003b_w s_z$.

The term s_{ze} is referred to as an "equivalent crack spacing factor" and has been developed to model the effects of different maximum aggregate size on the shear strength of concrete sections by modifying the crack spacing parameter. For concrete sections with less than the minimum quantity of transverse reinforcement and constructed with a maximum aggregate size of 20mm, s_{ze} is equal to s_z. For concrete with a maximum aggregate size other than 20mm, s_{ze} is calculated as follows:

$$s_{ze} = \frac{35s_z}{15 + a_g} \geq 0.85s_z \tag{7}$$

To account for aggregate fracturing at high concrete strengths, an effective maximum aggregate size is calculated by linearly reducing a_g to zero as f'_c increases from 60 to 70MPa. The term a_g is equal to zero if f'_c is greater than 70MPa. The square root of the concrete strength is limited to a maximum of 8MPa.

Since specimens with transverse reinforcement do not exhibit a size effect, s_{ze} is set equal to 300mm for specimens with at least the minimum quantity of stirrups as per Equation (8). This has the effect of reducing the size effect term to 1.

$$\frac{A_v f_y}{b_w s} = 0.06\sqrt{f'_c} \tag{8}$$

The angle of inclination of the cracks at the beam mid-depth, θ, is calculated by the following equation:

$$\theta = (29^\circ + 7000\varepsilon_x)(0.88 + s_{ze}/2500) \leq 75^\circ \tag{9}$$

Experimental Program

The preceding discussion has shown that considerable differences exist between the ACI shear design provisions and the SMCFT. In particular, the ACI method can not account for either the size effect or the aggregate effect. To investigate these differences, a series of ten large-scale and eight one-fifth scale-model shear-critical reinforced concrete beams were constructed and loaded to failure in the Mark Huggins Laboratory in the Department of Civil Engineering at the University of Toronto.

As summarized in Table 1 and Figure 2, the large beams measured 1510mm tall x 300mm wide x 9000mm long. Nine of the beams were reinforced with five No. 30 rebars in tension at an effective depth of 1400mm and with two No. 20 rebars for compression reinforcement. These beams were constructed without stirrups. The tenth large beam (specimen SB-10-H-S) was reinforced with eight No. 30 rebars in tension, two No. 20 rebars in compression, and approximately the minimum quantity of stirrups required by Equation (8) for the f'_c on the day of test. The stirrups were in the form of single legs of 9.5mm (3/8'') diameter rebars on alternating sides of the beam, spaced at 235mm. The one-fifth scale model beams measured 330mm tall x 122mm wide x 1800mm long. The reinforcement in nine of the small beams consisted of four 9.5mm diameter rebars at an effective depth of 280mm. The tenth scale-model beam (SSB-10-H-S) was reinforced in shear with 5mm smooth bars placed at 160mm on alternating sides.

Table 1: Summary of Experimental Program and Observations

Test Specimen	Specimen Properties					Experimental Observations				ACI Method		SMCFT Method		
	ρ_s (%)	$\frac{A_v f_y}{b_w s}$	f'_c (1) (MPa)	s_{ze} (mm)	$a_{g,eff}$ (mm)	P_{exp} (kN)	V_{exp} (2) (kN)	V_{exp} (3) (kN)	Δ_{ult} (mm)	V_{ACI} (kN)	$\frac{V_{exp}}{V_{ACI}}$	V_{SMCFT} (kN)	$\frac{V_{exp}}{V_{SMCFT}}$	ε_x (mm/m)
SB-10-N-1	0.83	0	38.4	1764	10	499	264	277	9.0	435	0.64	239	1.10	0.56
SB-10-N-2	0.83	0	40.3	1764	10	454	241	254	8.8	445	0.57	243	0.99	0.57
SB-10-H-1	0.83	0	73.6	2940	0	449	239	252	6.6	582	0.43	223	1.07	0.53
SB-10-H-S	1.33	0.50	71.2	300	0	1388	708	721	27.5	802	0.90	729	0.97	1.04
SB-20-N-1	0.83	0	31.4	1260	20	499	264	277	9.7	393	0.70	256	1.03	0.60
SB-20-N-2	0.83	0	33.2	1260	20	500	264	277	9.9	404	0.69	261	1.01	0.61
SB-40-N-1	0.83	0	28.1	1071	40	453	241	254	8.2	372	0.68	262	0.92	0.61
SB-40-N-2	0.83	0	28.5	1071	40	545	287	300	10.2	374	0.80	263	1.09	0.62
SB-50-N-1	0.83	0	41.0	1071	50	512	270	283	9.2	449	0.63	298	0.91	0.69
SB-50-N-2a	0.83	0	40.1	1071	50	565	297	310	9.4	444	0.70	295	1.01	0.69
SB-50-N-2b	0.83	0	40.1	1071	50	614	321	334	11.1	444	0.75	295	1.09	0.69
										Average:	0.68		1.02	
										Coefficient of Variation:	17.8%		6.6%	
SSB-10-N-1	0.83	0	41.9	353	10	72.7	36.6	36.8	3.5	36.9	1.00	32.5	1.13	0.90
SSB-10-N-2	0.83	0	41.9	353	10	76.1	38.3	38.5	3.9	36.9	1.04	32.5	1.18	0.90
SSB-10-H-1	0.83	0	77.3	588	0	74.9	37.7	37.9	3.2	47.3	0.80	33.6	1.12	0.93
SSB-10-H-S	1.34	0.50	77.3	300	0	132	66.3	66.5	7.7	67.3	0.99	59.6	1.11	1.03
SSB-20-N-1	0.83	0	39.2	252	20	77.7	39.1	39.3	3.5	35.7	1.10	33.4	1.17	0.93
SSB-20-N-2	0.83	0	38.1	252	20	75.9	38.2	38.4	3.5	35.2	1.09	33.1	1.15	0.92
SSB-40-N-1	0.83	0	29.1	214	40	83.3	41.9	42.1	6.2	30.8	1.37	31.0	1.35	0.86
SSB-40-N-2	0.83	0	29.1	214	40	69.3	34.9	35.1	3.9	30.8	1.14	31.0	1.13	0.86
										Average:	1.07		1.17	
										Coefficient of Variation:	15.1%		6.7%	

Notes:
(1) day of test
(2) Calculated at d_v=0.9d from face of loading plate, incl. self-weight
(3) Calculated at d from face of support, incl. self-weight

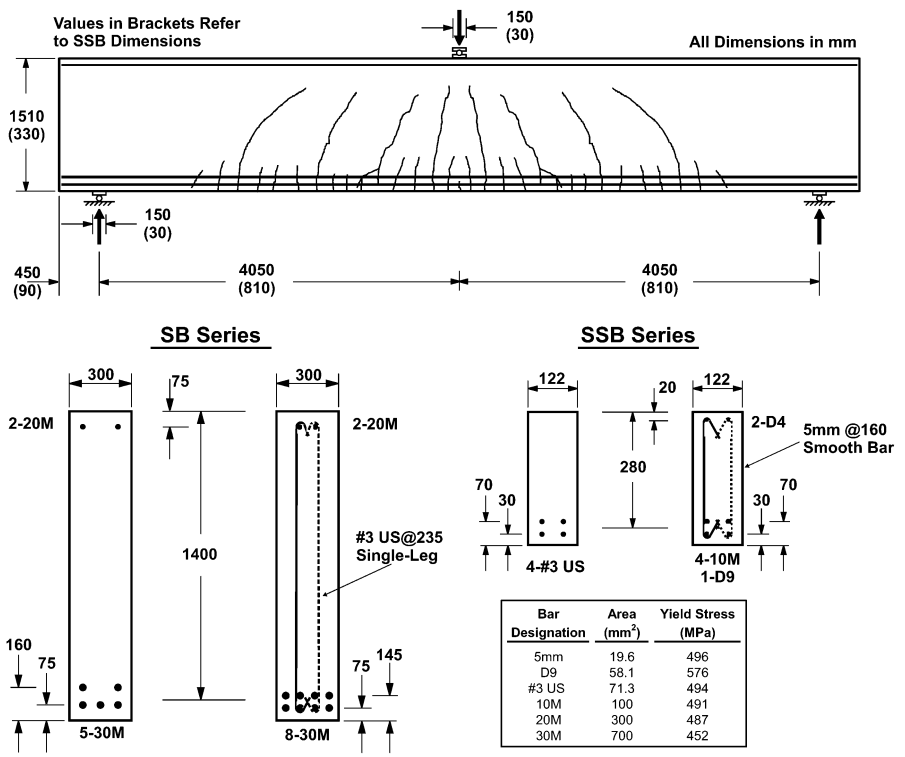

Figure 2: Specimen Design

The N series of beams were constructed with normal strength concrete and with four different maximum aggregate sizes (10, 20, 40 and 50mm). Two duplicate specimens were cast for each aggregate size. The H-series of beams were constructed with high-strength concrete and a maximum aggregate size of 10mm. The concrete used was commercially available from a local ready-mix supplier. The aggregate was strong crushed limestone shipped from a quarry on Manitoulin Island and conforming to CSA grading requirements.

The beams were moist-cured for five days, after which they were removed from their formwork. The beams were loaded to failure in three-point bending at an a/d ratio of 2.89. The large beams were tested in a 4500kN force-controlled Baldwin Test Frame, and the small beams were tested in a 1000kN displacement controlled MTS actuator (Figure 3). Upon reaching 85% of the monotonic failure load of the duplicate specimen, the applied load for beams SB-10-N-2 and SB-20-N-2 was cycled 20 times from 225kN to this load. This process was repeated at 90% and 95% of the monotonic failure load. After Specimen SB-50-N-2 failed on the east side of the beam (SB-50-N-2a), this side was clamped together with a series of externally installed Dywidag bars, and the beam was reloaded until failure occurred on the west end (SB-50-N-2b).

Figure 3: Specimen Test Setup

Experimental Results

Experimental results are summarized in Table 1 and typical load deflection curves are presented in Figure 4. All beams failed in shear prior to reaching their flexural capacity. The large beams without stirrups exhibited extremely brittle behaviour, failing at ratios of mid-span deflection to span of 1/750 or less. Failure was sudden and was preceded by relatively little cracking. The large beam with stirrups (SB-10-H-S) failed after a significant amount of cracking and deflection. Prior to failure, the failure shear crack reached a width of 4mm, and the Δ/L ratio was 1/300. The use of minimum stirrups and additional longitudinal steel increased the shear capacity by 2.9 times over the equivalent specimen without stirrups, providing a dramatic and beneficial effect on the shear strength of the section. The small beams all exhibited slightly greater ductility. The small beam with stirrups was the most ductile of all the specimens with a Δ/L ratio of 1/200. Like the equivalent large specimen, this beam was extensively cracked prior to failure. However, the use of minimum stirrups and additional longitudinal steel increased the shear capacity by only 1.8 times over the equivalent beam without stirrups. Thus, stirrups are far more effective for deep members than for shallow members.

The results shown in Figure 4 also indicate that the failure load generally increased for increasing aggregate size. The most likely explanation for this result is the increased surface roughness of the failure shear cracks caused by the larger aggregate. That is, failure was initiated at a higher shear stress in the

beams with large aggregate due to enhanced aggregate interlock capacity at the cracks. Note that Specimen SB-10-H-1, constructed with high-strength concrete, had the lowest peak load of all the large beams tested. This was due to reduced aggregate interlock caused by aggregate fracturing. In this case the effective aggregate size was 0mm.

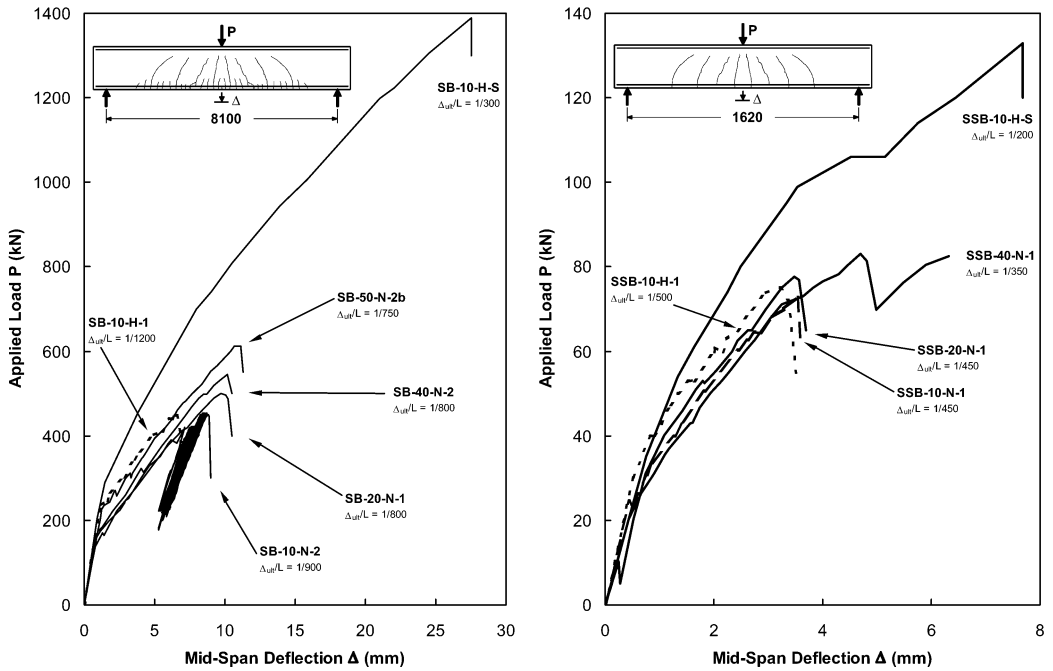

Figure 4: Typical Load-Deflection Curves of Test Specimens

The typical progression of failure in a large beam without stirrups is illustrated in Figure 5. These photos are of the shear critical region on the east side of Specimen SB-40-N-1 and were taken with a high-speed digital camera. The cracks have been digitally enhanced for clarity. In Figure 5a, the progression of cracks at 98% of the peak load is shown, and it can be clearly seen that a dominant flexural-shear crack has formed. The cause of the size effect is clearly demonstrated, in that the average longitudinal spacing of the cracks increases from 150mm at the level of the steel to 900mm at the beam mid-depth. In order to maintain a linear strain profile, these cracks are wider near the beam mid-depth than they are at the level of the steel. As the load is increased to the peak load, the dominant flexural shear crack extends slightly (5b). After the peak load has been reached, the dominant shear crack extends towards the loading point and widens (5c, 5d). After the dominant crack extends towards the load point, it also extends back towards the support point (5e) due to dowel forces in the longitudinal steel. At final failure, shown in Figure 5f, the failure crack is very wide and the bottom cover has been ripped from the bottom steel.

A Comparison of Methods

The failure shear predictions generated by the ACI Design Code and the SMCFT are summarized in Table 1. To account for the beam self-weight, it is appropriate, when using the ACI shear design method, to express the failure shear stress as the shear stress located at a distance d from the face of the support. When using the SMCFT, it is appropriate to calculate the failure shear at a distance d_v from the face of the loading plate. While the shear due to self-weight is slightly reduced, calculating the failure shear at this location takes into account the far more dominant effect of the moment on the longitudinal strain in the web, ε_x. The SMCFT produced safe and accurate failure shear predictions. The average ratio of experimental to predicted failure shear was 1.17 for the small beams, with a coefficient of variation of

6.7%. The average ratio of experimental to predicted failure shear was 1.02 for the large beams, with a coefficient of variation of only 6.2%. Comparison with the ACI predictions indicates that the ACI method has a lower experimental/predicted value for the small beams. Note, however, that the SMCFT is consistently conservative for the small beams over the entire range of aggregate sizes, resulting in a lower coefficient of variation. The increased scatter evident in the ACI predictions of the small beams shear strengths is indicative of an inability to properly account for the effects of the maximum aggregate size.

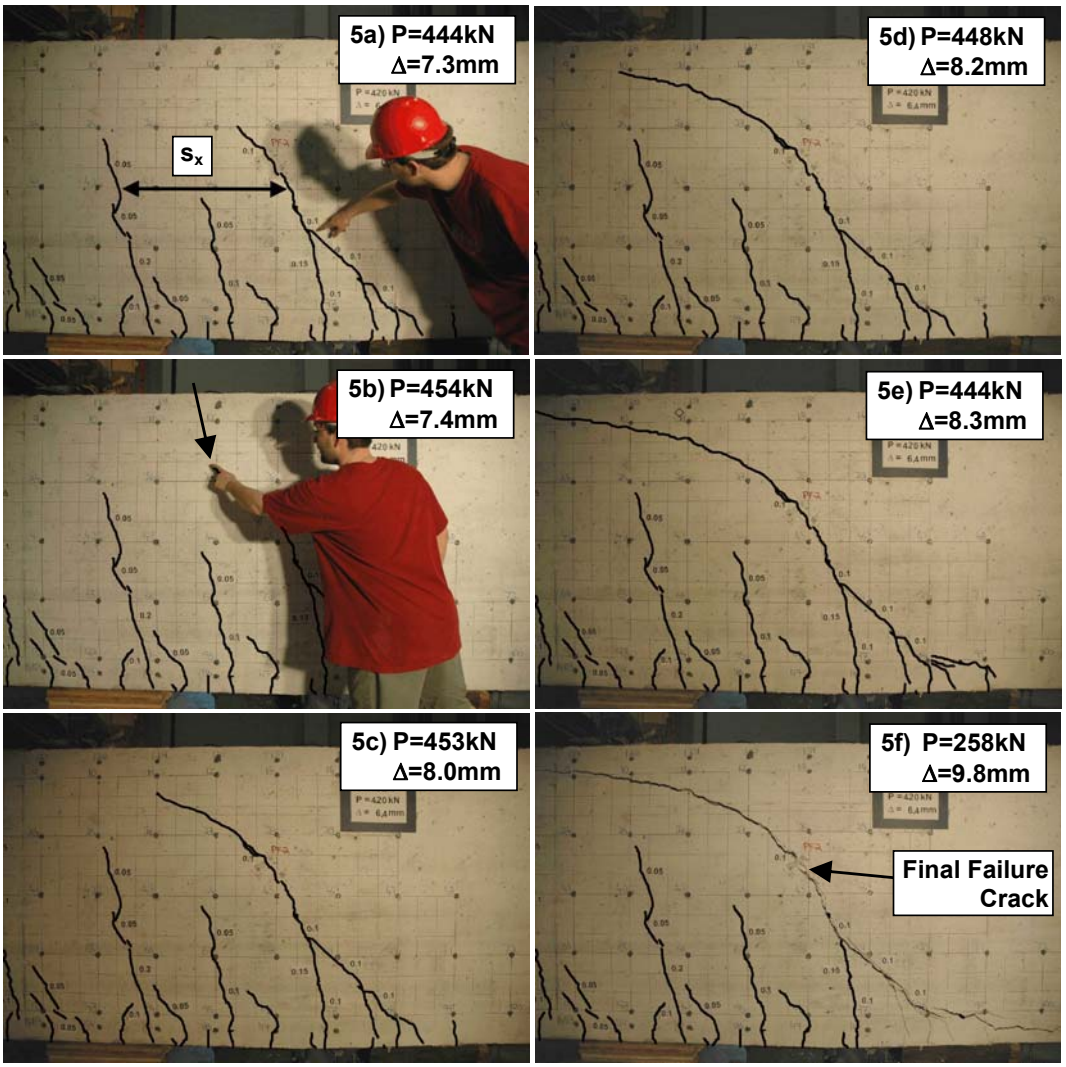

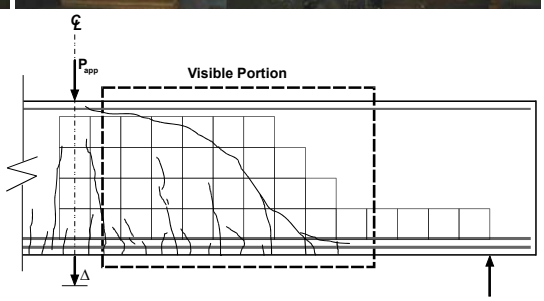

Figure 5: Progression of Failure Crack in Specimen SB-40-N-1

The ACI predicted failure shears for the large beams without stirrups ranged from 43% to 80% of the experimental failure shears. Clearly the ACI design method produces grossly unconservative predictions for large beams constructed without stirrups. Since the size effect is eliminated by the use of minimum stirrups, the ACI method produced an acceptable prediction of the failure shear stress of specimen SB-10-H-S. Despite the inability to account for aggregate effects, the ACI method produced otherwise excellent predictions of the failure shears of the scale model beams. This is to be expected, as the height of these beams was almost exactly the same as the average height of the beams tested to derive Equation (3).

Since the concrete strengths for all of the tested specimens varied, some thought is required to asses the true effect of the aggregate size. It is possible to normalize the experimental results by their concrete strengths and recalculate the experimental failure loads for the average f'_c of all the specimens (Sherwood, 2006). The normalized and recalculated experimental failure shears of the beams without stirrups are plotted in Figure 6 as a function of the aggregate size. The averages of duplicate specimens are shown, along with the experimental range at each aggregate size. This figure clearly and explicitly demonstrates that the shear strength increases as the aggregate size increases, but ceases to increase beyond an aggregate size of 25mm. The SMCFT successfully predicts the effects of the maximum aggregate size.

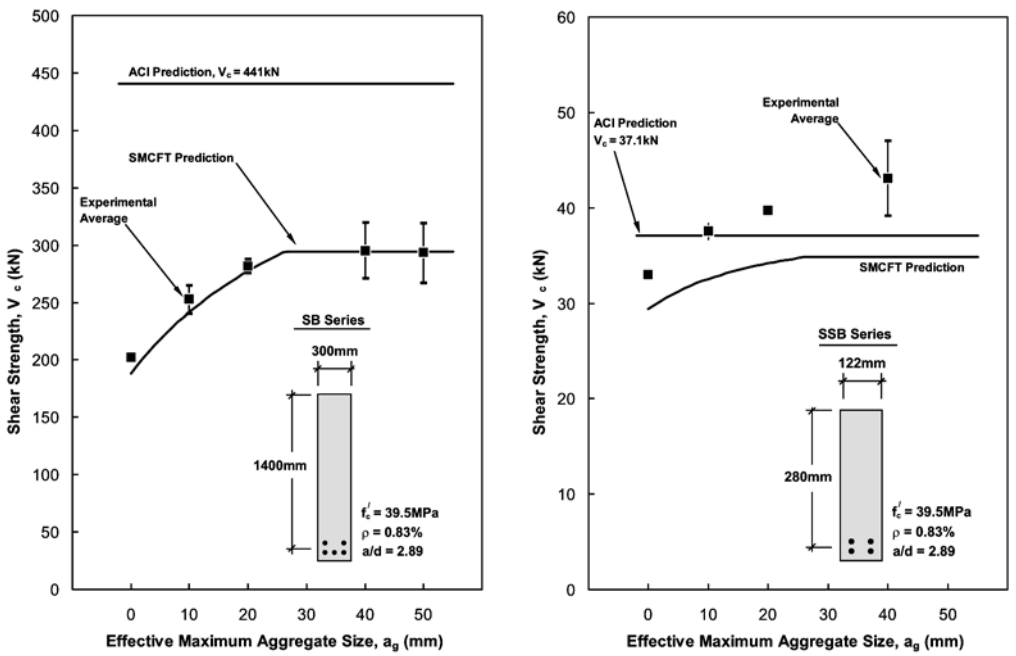

Figure 6: ACI and SMCFT Prediction of the Shear Strength of the Test Specimens

Since there is no difference between the shear behaviour of beams and one-way slabs, the large specimens can be thought of as 300mm sections taken from a wide, deep slab. If this slab was a large transfer element in high-rise construction, a likely ratio of dead load to live load would be 3:1 (Sherwood et al., 2005b), resulting in a safe service load of 60% of the failure load. As such, specimens SB-10-N-2 and SB-10-H-1 failed below the safe service load predicted by the ACI code. If a one-way transfer slab similar to these specimens designed by the ACI code were in use in a real structure, there would be a risk of failure under service loads, with little to no warning of impending collapse. The ACI method, however, is perfectly acceptable when designing shallow one-way slabs.

The Size Effect Factor

A unique aspect of the SMCFT is the introduction of the effective crack spacing parameter, s_{ze} (Equation 7). It is implemented into the expression for V_c through the size effect factor, $1300/(1000+s_{ze})$.

A wide range of effective crack spacings (from 214mm to 2940mm) was investigated in this study by varying only two variables: the effective depth and the maximum aggregate size. A graph showing the SMCFT predictions of the size effect factors for all of the beams tested is presented in Figure 7. Also shown are average experimental values of duplicate tests. The experimental points for the beams with stirrups are shown in white. The values of $V_{c,exp}$ for these two beams were calculated by subtracting the steel contribution calculated by Equation (4) from the total experimental failure shear force. This figure shows that the size effect factor can accurately model the shear strength of concrete sections over a wide range of both depths and aggregate sizes.

$$\frac{V_{c,exp}/b_w d_v}{\sqrt{f'_c}\,\frac{0.40}{(1+1500\varepsilon_x)}}$$

The effective crack spacing of 2940mm for Specimen SB-10-H-1 represents the highest value for s_{ze} ever tested. Basing the 2004 CSA shear design method on a rational theory rather than empirical relationships allows it to accurately predict the shear behaviour of a reinforced concrete beam in which an experimental variable was set outside the range of previous experimental data. It is also worthwhile to note that the experimental results for the beams with stirrups follow the trend of the equivalent beams without stirrups. It is therefore appropriate to use an s_{ze} value of 300mm for beams containing at least the minimum quantity of stirrups.

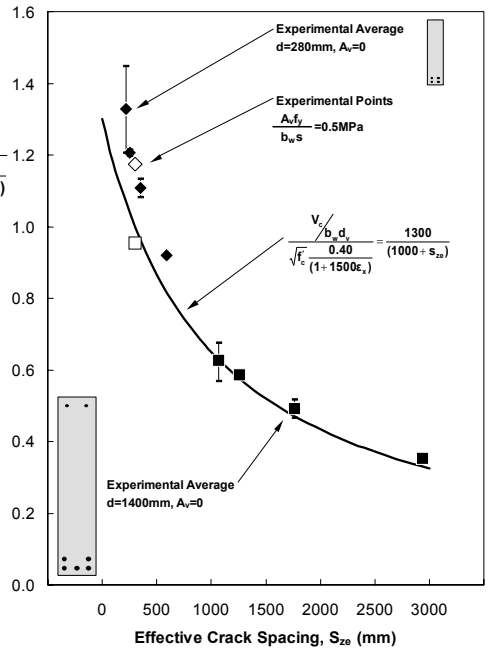

Figure 7: SMCFT Prediction of the Size Effect Term

Proportion of Shear Carried in Compression Zone

In order to definitively demonstrate the importance of aggregate interlock, the compression zone at the head of dominant shear cracks in several beams was instrumented with two columns of longitudinal concrete strain gauges. This was done with the intention of measuring the shear force carried by the compression zone.

As shown in Figure 8, the flexural strains measured by columns of gauges spaced at 80mm on the 365mm deep compression zone of Beam SB-10-N-2 allowed for the calculation of adjacent flexural stress profiles. Equilibrium requires that a horizontal complimentary shear stress of $v = \Delta C/(b_w \times 80)$ act at every level of the compression zone. Equilibrium further requires that the vertical shear stress equals the horizontal shear stress at every level of the compression zone. This allows for the vertical shear stress distribution to be calculated, as shown in Figure 8. The total shear force acting in the compression zone is therefore equal to $V = \int_A v \cdot dA$. For the shear stress distribution shown in the figure, the shear force carried in the compression zone is 50kN, representing 24% of the total shear force acting at the section. Clearly, then, 76% of the remaining shear must be carried by aggregate interlocking along the dominant shear crack and dowel forces. However, the shear crack is vertical at the level of the steel, indicating that the dowel forces transferred by the longitudinal reinforcement are extremely small.

Concluding Remarks

The ACI design code is dangerously unconservative when applied to the shear design of large concrete beams and one-way slabs constructed without stirrups. The ACI method is capable of accurately predicting V_c of members without stirrups only if their height is similar to the original experimental set used to calibrate the equation. To provide an adequate level of safety, the current ACI equation for V_c must be replaced with an expression that can account for the size effect in shear.

The primary mechanism of shear transfer in slender beams constructed without stirrups is aggregate interlock. It is incorrect to assume that the entire shear force is transferred in the compression zone. Clearly, then, any shear design provision that claims to be theoretically sound must be based on a theory that recognizes the critical importance of aggregate interlock in shear transfer. In this regard, the SMCFT represents a clear improvement over the ACI method.

The risks of basing design code provisions on empirical relationships rather than sound theory have been demonstrated in this paper. Developers of structural design codes owe it to the profession to base provisions wherever possible on rational theory rather than risky empiricism.

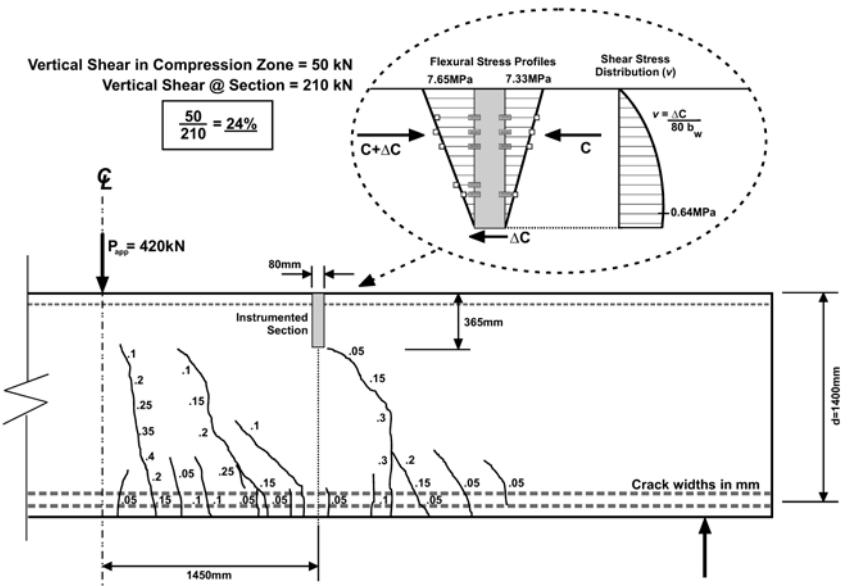

Figure 8: Calculation of Shear Carried in Uncracked Compression Zone, Specimen SB-10-N-2

References

ACI Committee 318 (2005) *Building Code Requirements for Structural Concrete (ACI 318-05) and Commentary*, American Concrete Institute, Farmington Hills, MI, USA

ACI-ASCE Committee 326 (1962) "Shear and Diagonal Tension," *ACI J., Proc.*, **59**: 1-30, 277-344, 352-396

Bazant, Z., Yu, Q. (2005) "Designing Against Size Effect on Shear Strength of Reinforced Concrete Beams Without Stirrups," *ASCE J. Struct. Engrg*, **131**(12) "I: Formulation" 1877-1885, "II: Verification and Calibration" 1886-1897

Bentz, E.C., F.J. Vecchio and Collins, M.P. (2005) "The Simplified MCFT for Calculating the Shear Strength of Reinforced Concrete Elements, *ACI Struct. J.*, submitted April 2005, 45pp.

CSA Committee A23.3. 2004. *Design of Concrete Structures (CSA-A23.3-04)*, Canadian Standards Association, Rexdale, ON

Fenwick, R.C. and Pauley, T. (1968) "Mechanisms of Shear Resistance of Concrete Beams," *ASCE Struct. J.,* **94**(ST10): 2235-2250

Lubell, A., Sherwood, T., Bentz, E. and Collins, M.P. (2004) "Safe Shear Design of Large, Wide Beams," *Concrete International*, January, **26**: 66-78

Mörsch, E. 1909. Concrete-Steel Construction. McGraw Hill Inc., New York, NY, USA

Sherwood, E.G., Bentz, E. and Collins, M.P. (2005a) "The Behaviour of Large, Lightly Reinforced Concrete Beams and One-Way Slabs," CSCE Annual Conference, Toronto, Ontario, June 2-4, 2005, Paper GC-167

Sherwood, E.G., Lubell, A., Bentz, E. and Collins, M.P. (2005b) "One-Way Shear Strength of Thick Slabs," *ACI Struct. J.*, 40pp., submitted July 2005

Sherwood, E.G. (2006) *Behaviour and Design of Large, Lightly-Reinforced Concrete Flexural Elements Subjected to Shear*, Ph.D. Thesis, University of Toronto, *in progress*

Tureyn, A.K. and Frosch, R.J. (2003) "Concrete Shear Strength –Another Perspective," *ACI Struct. J.*, **100**(5): 609-615

Vecchio, F and Collins, M.P. (1985) "The Modified Compression-Field Theory for Reinforced Concrete Elements Subjected to Shear," *ACI Journal*, **83**(2): 219-231